Global NEST Journal, Vol 15, No 2, pp 227-240, 2013

ESTIMATION OF POLLUTION DISPERSION PATTERNS OF A POWER PLANT PLUME IN COMPLEX TERRAIN

DELIGIORGI D. *
PHILIPPOPOULOS K.
KARVOUNIS G.

National and Kapodistrian University of Athens,
Department of Physics,
Division of Environmental Physics and Meteorology
Panepistimioupolis, GR-15784 Athens, Greece

Received: 05/04/13
Accepted: 22/04/13

*to whom all correspondence should be addressed:
e-mail: despo@phys.uoa.gr

ABSTRACT

This study aims to identify the pollutant dispersion patterns in complex terrain under various meteorological conditions. The study area is situated at Chania plain on the island of Crete, Greece, where the topography is fairly complex. Thus, the local meteorology is expected to be deeply affected by this complex morphology. The main source of air pollution in the region is a diesel power generating plant. The daily averaged ground level distributions of sulfur dioxide, emitted from the power plant, were predicted using the AERMOD modeling system. In order to assess the meteorological conditions in the wider region, a meteorological monitoring network with six stations was installed and operated for two years. A detailed spatial and temporal analysis of the meteorological parameters is performed in order to determine their ability to characterize the transport and dispersion conditions in the area of concern. The model was applied for days with well established wind flows and the case studies indicate that such a model is capable of predicting the general pattern of ground-level concentrations of sulphur dioxide in the area of the power plant.

KEYWORDS: Air quality, dispersion modeling, atmospheric stability, wind, mixing height, complex topography, synoptic flow effects.

1. INTRODUCTION

Air quality deterioration is related to the capability of the atmosphere to disperse pollutants and to the energy production and consumption patterns in the area under investigation. Air pollution modeling is a method for providing information on air quality in a region based on what we know of the emissions, and of the atmospheric processes that lead to pollutant dispersion and transport in the atmosphere (Moussiopoulos *et al.*, 2000; Borrego *et al.*, 2003; San Jose *et al.*, 2006; Gualtieri *et al.*, 2008; Davitashvili, 2009). In most air quality applications, the main concern is the dispersion in the Planetary Boundary Layer (PBL), the turbulent air layer next to the earth's surface that is controlled by the surface heating and friction and the overlying stratification. The key issues to consider in air pollution modeling are the complexity of the dispersion, which is controlled by terrain and meteorology effects along with the scale of the potential effects (e.g. human health) (Bluett *et al.*, 2004).

Air pollution models are classified according to the scales of application. Short-range models apply to spatial scales up to ten kilometers, while urban and long-range transport models to larger scales. The most widely used models for predicting the impact of relative inert gases, such as sulfur dioxide, which are released from industrial point sources, are based on the Gaussian diffusion (Venkatram, 2001). A Gaussian plume model assumes that if a pollutant is emitted from a point source, the resulting concentration in the atmosphere, when averaged over sufficient time, will approximate a Gaussian distribution in vertical and horizontal directions (Turner, 1964; Briggs, 1971; 1972). The

Gaussian models require meteorological data from a single meteorological station and assume this data to be applicable for the entire modeling domain.
This paper, initially, discusses representivity issues of measured and estimated meteorological parameters which are used as inputs in such models when applied to inhomogeneous terrains. The limitations associated with the use of Gaussian models in complex topography involve a determination of a sub-area with uniform meteorological and dispersion conditions. The ground level distributions of sulfur dioxide (SO_2) on a daily averaging period basis, emitted from the power plant, were predicted using the AERMOD modeling system, which incorporates all the current understanding of dispersion and micrometeorology, to model the impact of point sources at short distances. The surface pressure maps of the Southeastern Mediterranean region at 00:00 UTC along with the meteorological measurements of the station network are used for the selection of days and to characterize the weather conditions in the region. In detail, the identification of the distinct meteorological conditions with well established wind flows in the region is performed by analyzing the daily evolution of wind speed and direction from the experimental measurements, with increased significance the measurements from the station of Souda, due to its proximity to the modeled power plant.

2. EXPERIMENTAL AREA AND DATA

The study area is at the southeastern part of the Chania plain, located on the island of Crete, Greece (Figures 1 and 2). The greater area is constricted by physical boundaries. These are the White Mountains on its southern side and the Aegean coastline on its northern and eastern part. The topography of the region is characterized fairly complex due to the proximity to the sea and also because of the hills which rise sharply into mountainous heights. The region's topography, land-use, along with the existence of a single significant air pollution point source makes the area suitable for identifying the dispersion patterns in complex terrain under various meteorological conditions.
The diesel power generating plant, operated by the Public Power Cooperation S.A. of Greece (PPC), with seven stacks of different technical and operational specifications, is situated in a suburban area, on the outskirts of the city of Chania and is the main source of air pollution in the region (Figures 1 and 2). In order to assess the meteorological conditions in the greater region and more specifically in the modeling domain, a meteorological network of six stations (Figure 1) has been used for two years (August 2004 to September 2006). These stations cover the main topographical features and land-use characteristics of the region. The station sites cover the main topographical and land-use characteristics of the study area (Table 1). Table 2 summarizes the available surface meteorological observations in each station. Upper air measurements are provided from atmospheric soundings at the civil airport of Heraklion. Surface weather maps of the Southeastern Mediterranean region at 00:00 UTC and 12:00 UTC are available from the Hellenic Meteorological Service (HMS).

Table 1. Characteristics of the meteorological stations

Station (Abbreviation)	**Altitude (m)**	**Station Type**
Souda (SOU)	118	Suburban
Platanias (PLA)	23	Rural – Coastal
Malaxa (MAL)	556	Rural – Inland
TEI (TEI)	38	Urban – Coastal
Airport (AER)	140	Rural
Pyrovoliko (PBK)	422	Rural

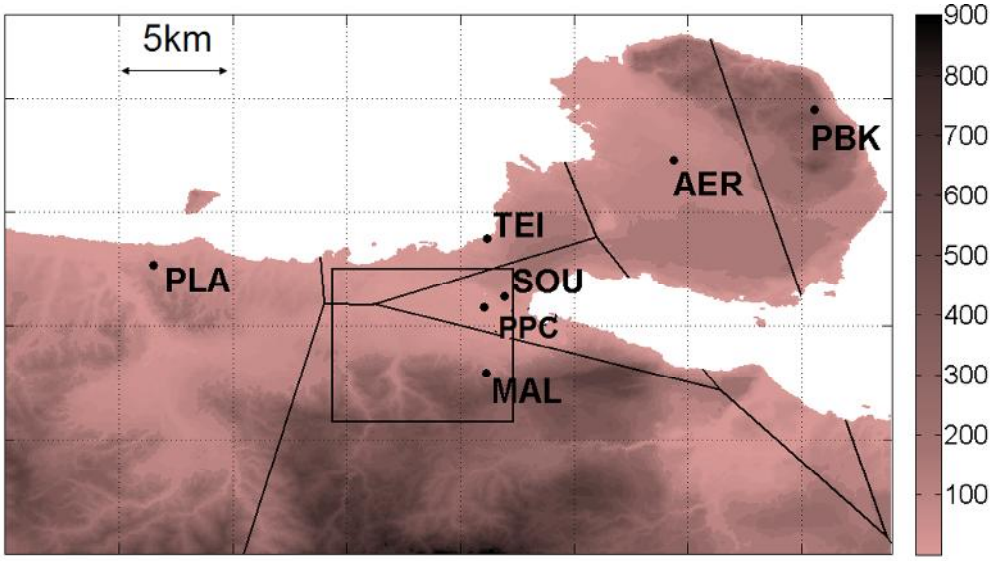

Figure 1. Study Area, meteorological stations network, spatial proximity polygons of the meteorological stations and modeling domain

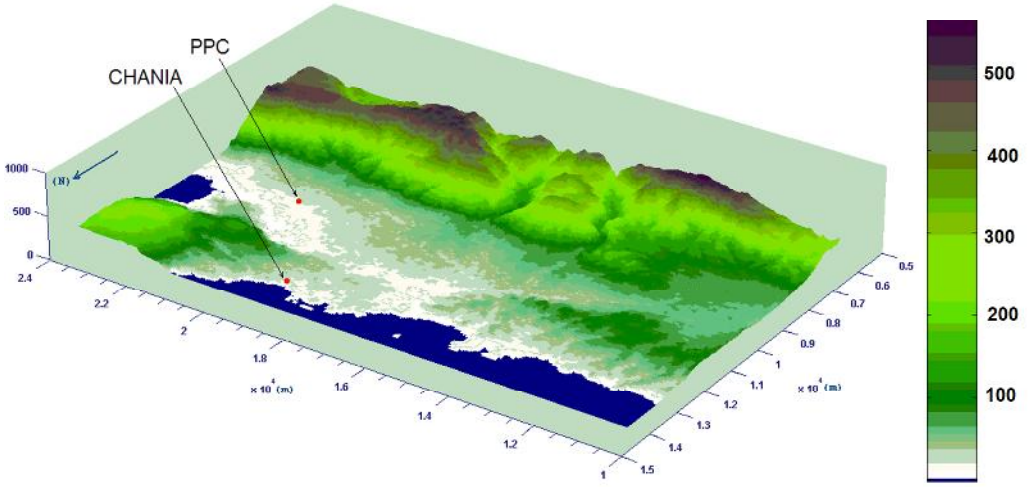

Figure 2. 3D visualization of the study region
(rotated map to show the physical boundaries of Chania plain)

Table 2. Measured meteorological parameters

Meteorological Parameter	PLA	SOU	MAL	TEI	AER	PBK
Temperature (^{o}C)	✓	✓	✓	✓	✓	✓
Relative Humidity (%)	✓	✓	✓	✓	✓	✓
Atmospheric Pressure (hPa)		✓		✓		✓
Wind Speed (m sec^{-1})	✓	✓	✓	✓	✓	✓
Wind Direction (^{o})	✓	✓	✓	✓	✓	✓
Rainfall (mm)		✓	✓	✓	✓	✓
Soil Temperature (^{o}C)	✓	✓		✓		
Cloud Cover (%)					✓	
Solar Radiation (W m^{-2})				✓		
Net Radiation (W m^{-2})				✓		
Ceiling Height (ft)					✓	
Sunshine Duration (hr)					✓	

3. HOMOGENEITY ASSESSMENT OF METEOROLOGICAL PARAMETERS

Topography, as well as in-homogeneity of thermal and dynamic properties of the surface, causes distortion of atmospheric flow and turbulence. Air flow in dispersion modeling is typically parameterized by measurements of wind, and turbulence by atmospheric stability and mixing height. An extensive meteorological network enables the assessment of the spatial meteorological homogeneity in a region with complex topographical features.

3.1 Wind Speed and Direction Assessment

A qualitative analysis of wind field homogeneity can be performed by plotting each station's observations in the u-v plane, where each wind speed vector is represented by a single point. The local point density can be calculated by using the Kernel Density Estimation (Hazelton and Turlach, 2007), which in our case is expressed by the following formula:

$$\hat{f}_h(\vec{x}) = \frac{1}{N h^2} \sum_{i=1}^{N} G\left(\frac{\vec{x} - \vec{x}_i}{h} \right)$$

where G is the two-dimensional Gaussian distribution, h the Kernel band-width and $\mathbf{x}_1,\ldots,\mathbf{x}_N$ the observations. The resulting diagrams, which can be considered as an alternative representation of wind roses, are presented for all stations in Figure 3.

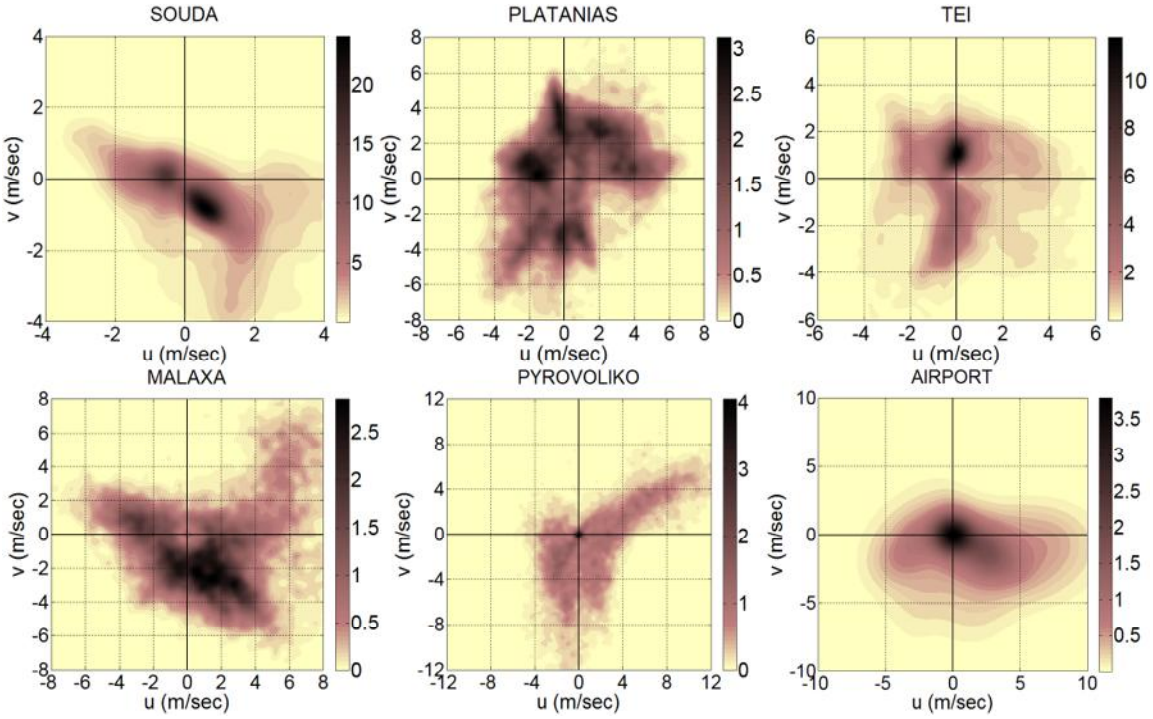

Figure 3. Gaussian Kernel density estimation of wind vectors, using a 0.2 bandwidth. The color-scales correspond to point density, measured in percentage of points per $(\text{m sec}^{-1})^2$

From these plots, the in-homogeneity of the wind field along with the exposure of each station to different local conditions is apparent. By examining the densities of the SOU and MAL stations, which are geographically proximate, a two peak distribution is observed. However, it is observed a considerable scatter at the MAL station which is attributed to differences in altitude and terrain. The considerable differences in their prevailing wind directions between the SOU and the TEI stations are due to the proximity of the TEI station to the Aegean coastline and thus, its observations are highly affected by sea and land breeze circulations. PLA measurements exhibit considerable scatter and are mainly influenced by downslope winds, while the PBK station is mainly influenced by upslope winds due to its location (elevated station in the North-Eastern part of the Chania peninsula). AER station observations are mainly affected by Northwesterly winds as a mountain barrier located to the Northeast blocks the Northeasterly flow.

A quantitative similarity test for the wind time series (Figure 4) is performed by using the similarity curves. They calculate percentages of similar concurrent observations between two time series. The notion of similarity is expressed through parameter R, which is used to define whether two observations are considered to be similar. Their formulation is described in the equation below:

$$s_{ab}(R) = \frac{1}{N}\sum_{i=1}^{N} I_i \quad \text{where} \quad I_i = \begin{cases} 1 & \left\| \vec{v}_{a,i} - \vec{v}_{b,i} \right\| \le R \\ 0 & \text{otherwise} \end{cases}$$

where $\vec{v}_{a,1}, \vec{v}_{a,2}, ..., \vec{v}_{a,N}$ and $\vec{v}_{b,1}, \vec{v}_{b,2}, ..., \vec{v}_{b,N}$ is the first and second time series respectively and $s_{ab}(R)$ represents the percentage of pairs $(\vec{v}_{a,i}, \vec{v}_{b,i})$ with a distance less than R.

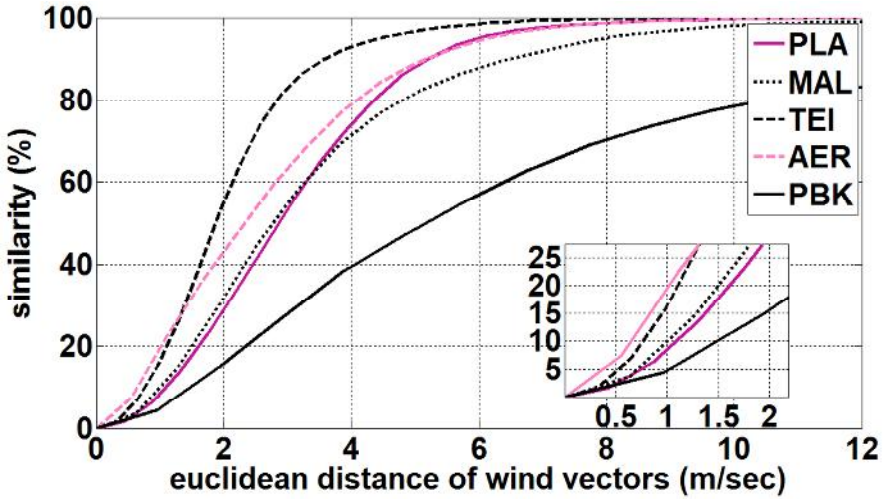

Figure 4. Similarity curves for SOU station

The above curves indicate a poor agreement between each station and SOU. For a tolerance of less than 1.3 m sec^{-1}, SOU station observations are similar to those of AER station with a percentage of 27%. By selecting higher tolerance values the TEI station exhibits the best overall similarity.

3.2 Atmospheric Stability Assessment

The most common stability classification scheme is the Pasquill-Gifford (P-G), which defines six stability classes namely A (highly unstable), B (moderately unstable), C (slightly unstable), D (neutral), E (moderately stable), and F (extremely stable). Stability class G was added to the initial scheme, to represent low wind night-time stable conditions (Pasquill, 1961). Several methodologies exist for the estimation of the P-G stability classes. In our study, initially, we compared the Turner and Sigma-A schemes for two monitoring stations (Table 3). The first method uses solar altitude, total cloud cover and ceiling height to calculate the Net Radiation Index (NRI), which in combination with wind speed gives the estimate of the stability classes (Turner, 1964). The Sigma–A method is a turbulence-based method which uses the standard deviation of the wind direction. Corrections to the initial stability class estimations are applied based on daytime and night-time conditions and mean wind speeds (Bailey, 2000).

The overall agreement of the two methodologies is 42.3% for the SOU station and 40.7% for the PLA station. These low percentages, along with the considerable variation of the Sigma-A results, with respect to Turner, exhibit the inconsistency of the two schemes. This disagreement can be attributed to the fact that the Sigma-A method is more sensitive to local topographical features which highly affect the standard deviation of wind direction. This fact has serious implications in terms of concentration predictions using Gaussian models.

Table 3. Variance (%) of the Sigma-A results with respect to Turner for SOU and PLA stations

SOU		Sigma-A						PLA		Sigma-A					
		A	B	C	D	E	F			A	B	C	D	E	F
Turner	**A**	74.6	16.1	8.4	0.9	--	--	Turner	**A**	34.8	31.4	27.5	6.3	--	--
	B	50.8	23.5	19.8	5.9	--	--		**B**	27.9	33.8	31.9	6.4	--	--
	C	46.8	16.4	28.4	8.5	--	--		**C**	18.4	20.9	44.2	16.6	--	--
	D	22.1	15.7	23.6	25.8	2.4	10.4		**D**	6.0	7.7	19.9	60.5	4.6	1.3
	E	5.4	4.6	4.7	37.0	18.3	30.1		**E**	1.6	2.4	5.5	61.2	19.1	10.3
	F	6.7	1.6	1.7	16.8	13.2	60.0		**F**	4.4	2.1	2.5	34.9	21.4	34.7

In order to examine the effect of the topography, land use and local flows on the turbulent state of the atmosphere in the region under study, the hourly evolution of atmospheric stability is studied for each station (Figure 5).

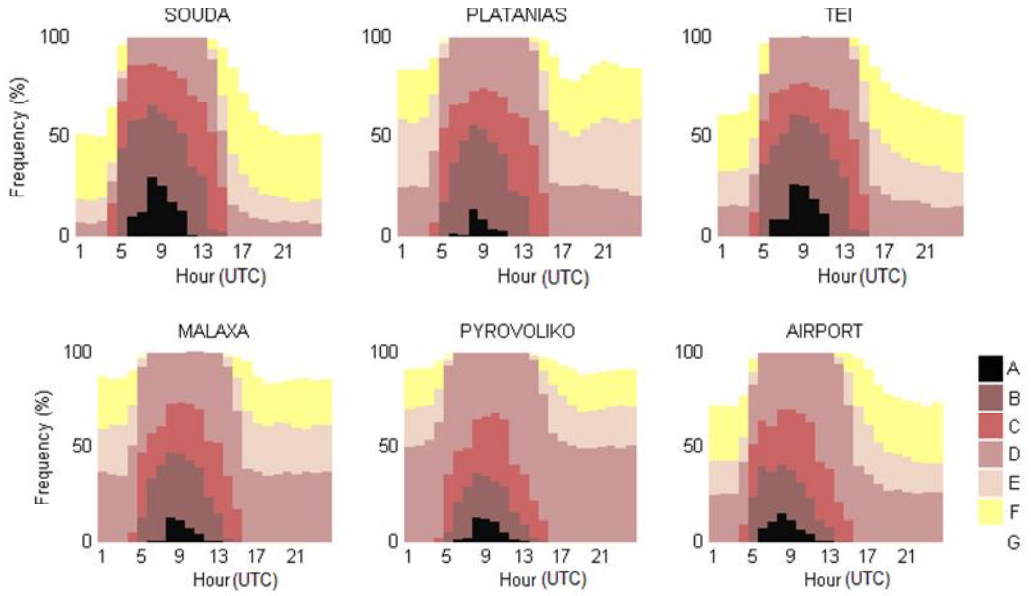

Figure 5. Hourly frequency distribution of atmospheric stability classes for each station

The analysis shows that all stations follow a general daily pattern, where stable conditions prevail during the night and unstable during the daytime. Higher occurrences of extremely stable and highly unstable conditions are observed at the urban station of TEI and the suburban SOU station. Furthermore, the unstable conditions for these two stations persist until later in the afternoon compared to the other stations.

In order to assess the spatial homogeneity of atmospheric stability in the region under study, tables of joint frequencies for all possible pairs of stations are calculated. For this analysis we used the Turner scheme for calculating stability classes. In Table 4 we present the findings for SOU station.

All stations show a wide variation of stabilities, spreading over 4 categories lower or higher in comparison with SOU station. High agreement is observed only for neutral conditions (D). The TEI station exhibits the best agreement with percentages ranging from 60% for extremely unstable conditions (A) to 88.2% for neutral conditions (D).

Table 4. Joint–frequencies of occurrence (%) of stability classes compared to SOU station

		PLA							MAL						
		A	**B**	**C**	**D**	**E**	**F**	**G**	**A**	**B**	**C**	**D**	**E**	**F**	**G**
SOU	**A**	**23.2**	69.8	6.9	0.1	--	--	--	**27.3**	59.9	12.5	0.3	--	--	--
	B	1.7	**59.8**	34.4	4.2	--	--	--	1.2	**48.3**	40.5	9.9	--	--	--
	C	0.0	7.1	**52.2**	40.6	--	--	--	0.0	3.5	**42.6**	53.9	--	--	--
	D	--	0.0	6.1	**89.6**	4.0	0.4	--	--	--	1.8	**97.4**	0.5	0.2	--
	E	--	--	--	50.3	**39.6**	9.5	0.5	--	--	--	83.8	**12.3**	3.5	0.4
	F	--	--	--	30.0	42.6	**23.9**	3.4	--	--	--	44.9	36.0	**17.4**	1.7
	G	--	--	--	1.6	24.5	41.7	**32.2**	--	--	--	6.8	26.4	40.2	**26.6**
		TEI							**AER**						
		A	**B**	**C**	**D**	**E**	**F**	**G**	**A**	**B**	**C**	**D**	**E**	**F**	**G**
SOU	**A**	**60.0**	38.4	1.6	--	--	--	--	**27.9**	46.8	25.3	--	--	--	--
	B	10.8	**71.6**	16.8	0.8	--	--	--	6.3	**38.5**	42.7	12.6			--
	C	0.2	14.4	**57.2**	28.2	--	--	--	0.3	2.6	**40.4**	56.6	--	--	--
	D	--	0.1	7.6	**88.2**	3.7	0.5	--	--	--	1.3	**97.9**	0.6	0.1	--
	E	--	--	--	37.4	**47.7**	12.7	2.1	--	--	--	78.5	**17.4**	4.0	0.1
	F	--	--	--	13.6	34.8	**42.9**	8.7	--	--	--	28.4	36.5	**34.3**	0.8
	G	--	--	--	0.4	3.0	26.7	**69.9**	--	--	--	1.2	10.1	38.7	**50.1**

		PBK							
		A	**B**	**C**	**D**	**E**	**F**	**G**	**UNDEFINED**
SOU	**A**	**22.8**	34.9	27.5	1.7	--	--	--	13.1
	B	3.8	**26.4**	37.2	20.9			--	11.6
	C	0.2	2.7	**24.6**	58.5	--	--	--	13.9
	D	--	--	1.7	**80.5**	0.1	0.1	--	17.5
	E	--	--	--	73.5	**5.4**	1.6	0.1	19.4
	F	--	--	--	55.7	16.6	**10.7**	0.7	16.3
	G	--	--	--	19.9	26.2	25.7	**15.9**	12.2

3.3 Mixing Height Assessment

Atmospheric mixing height is the depth of the layer which is characterized by strong turbulent and convective mixing (Ulke and Mazzeo, 1998). Owing to the lack of upper air measurements, the experimental Nozaki model (Cheng *et al.,* 2001) is adopted. It uses ground-level, routinely measured meteorological parameters. The mean hourly mixing height is estimated by the following formula (Cheng *et al.*, 2001):

$$H = \frac{121 \cdot (6 - P) \cdot (T - T_d)}{6} + \frac{0.169 \cdot P \cdot (U + 0.257)}{12 \cdot f \cdot \ln(z / z_o)}$$

where H is the mean hourly mixing height in meters, P a meteorological parameter that depends on P-G stability class, T the ambient temperature, T_d the dew point temperature, U the wind speed at 10m, f the Coriolis parameter and z_o the surface roughness length.

In order to assess the spatial homogeneity of the mixing height, we employed the same methodology that used for the wind vector (similarity curves). Results of the SOU station are presented in Figure 6.

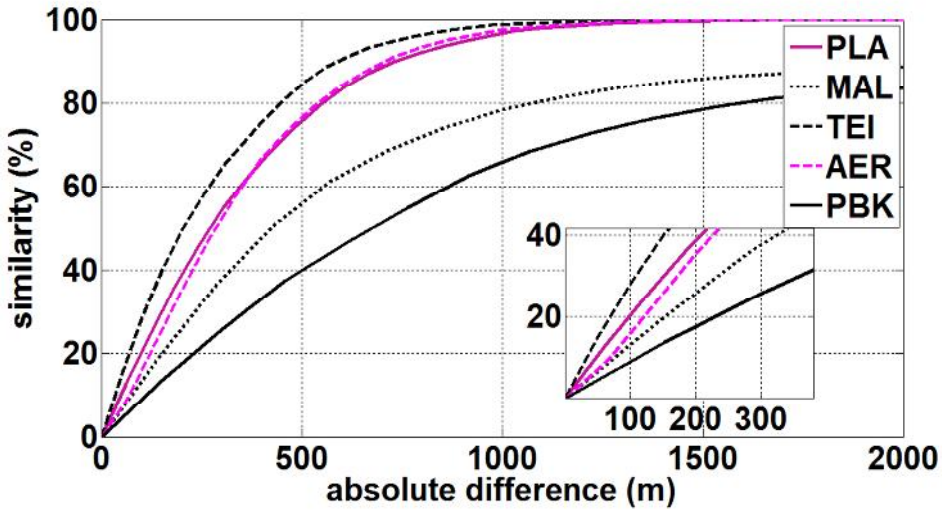

Figure 6. Similarity Degree of estimated Hourly Mixing Heights with respect to SOU station

From Figure 6, it can be seen that the TEI station gives the most consistent estimations of mixing height in comparison to SOU. Furthermore, the similarity of the neighboring SOU and MAL stations is less than that of SOU and PLA or AER. Thus confirming the highly in-homogeneity character of the area attributed to the intense topography which prevails in the South.

4. CASE STUDIES USING AERMOD MODELING SYSTEM

4.1 AERMOD modeling system

The AERMOD modeling system, developed by the American Meteorological Society and the U.S. Environmental Protection Agency, consists of two pre-processors and the dispersion model. AERMET, AERMOD modeling system's meteorological pre-processor, provides the dispersion model with the meteorological information it needs to characterize the PBL. AERMET uses routinely measured meteorological data (i.e. wind speed and direction, ambient temperature and cloud cover), surface characteristics (i.e. Albedo, Bowen ratio and Surface Roughness Length that they are not directly measured at the meteorological stations and a subjective estimation is often necessary) and upper air sounding data, to calculate boundary layer parameters (i.e. mixing height z_i, friction velocity u_*, Monin-Obukhov length L, convective velocity scale w^*, temperature scale θ^* and surface heat flux H). AERMAP, the terrain pre-processor, characterizes the terrain, using a Digital Elevation Model and generates receptor grids for the dispersion model. Furthermore, for each receptor grid (x_i,y_i) it generates a representative terrain-influence height H_c. This information along with the receptor's location and height above mean sea level (x, y, z), are forwarded to the dispersion model. The dispersion model in the Stable Boundary Layer assumes both the vertical and horizontal distributions to be Gaussian. In the Convective Boundary Layer the horizontal distribution is also assumed to be Gaussian, but the vertical distribution is described by a bi-Gaussian probability density function. The AERMOD modeling system may be used for flat and complex terrains as it incorporates the concept of a critical dividing streamline (Cimorelli *et al.*, 2004; Holmes and Morawska, 2006; Karvounis *et al.*, 2007).

Steady - state Gaussian - plume models and therefore AERMOD modeling system require meteorological data from a single surface meteorological station. Although on-site meteorological data are preferred, it is possible to use observations from an off-site station, given that the representativeness of the data is established before they are used in air dispersion modeling. Representativeness is the extent to which a set of measurements taken in a space-time domain reflects the actual conditions in the same or different space-time domain taken on a scale appropriate for a specific application (Nappo *et al.*, 1982; Latini *et al.,* 2002). Off-site data could be used in cases where the nearby site has similar topographic characteristics, which are likely to result in similar meteorological conditions for the air dispersion modeling area (Bluett *et al.*, 2004).

In our case the two–year experimental dataset is compared with the 50-year climatological data series provided by the HMS and the dataset is found to be a statistical representative sample of the

meteorological conditions that occur in the area of study (Deligiorgi *et al.,* 2009a). As it is shown above the greater area of Chania plain exhibits poor meteorological homogeneity and thus, a single representative station for the whole region cannot be selected. Thiessen polygons are initially employed to examine the spatial proximity of the available stations to the PPC power plant (Figure 1), identifying the region of spatial representativeness (based solely on distance) of each station. SOU station is representative of the PPC power plant region due to its proximity and resemblance in elevation, land-use, land-cover and topographical characteristics. Whereas, the proximity of the meteorological monitoring site is an important factor, representativeness is not simply a function of distance. Wind direction and speed influence the horizontal representativeness by enlarging it towards the predominant wind direction (Knoderer, 2004). In our case, the area corresponding to the SOU station can be extended southwesterly, following the prevalent wind direction. The proximity to the sea towards the west is expected to significantly alter the results and thus, our modeling domain extends 1km to the west, east and the north of the power plant and 2km to the south (Figure 1). Wind speed, wind direction and ambient temperature hourly values are obtained from the SOU station and are used as a meteorological input in the AERMOD modeling system. Cloud cover observations have greater spatial representativeness and are acquired from the more distant climatological AER station. Additionally, the required upper air observations are obtained from Heraklion site, which is the only station at the island of Crete that performs atmospheric soundings.
We applied the model to estimate daily averages of sulphur dioxide ground-level concentrations, under various anemological conditions. Once the representative days are selected, surface daily averaged concentrations of sulfur dioxide are estimated using AERMOD modeling system. Sulfur dioxide is selected as the pollutant of reference because due to its rather inert nature it is suitable to estimate the dispersion patterns in the region.

4.2 Case studies

According to Deligiorgi *et al*. (2008, 2009b) the atmospheric circulation over Southeastern Mediterranean and Greece can be classified into ten distinct patterns, which by taking into account the anemological conditions specifically over the Chania plain can be further grouped into six types. The air dispersion modeling is focused on the two more frequent types, which contain cases with medium to high intensity northerly flow (Type A – 13.32%) and smooth field or weak high-low pressure system interactions (Type B – 66.36%). According to the latter type the background synoptic gradient wind is rather weak, facilitating the development of local scale flows. Two case studies of Type A days (Figure 7) and four cases of Type B days (Figure 8 and 9) with different characteristics are presented.

For each case the surface pressure map along with the daily wind evolution at the station of SOU is illustrated. The ground level, daily averaged SO_2 concentrations are presented for each case study. In order to study the lower concentrations in more detail, the logarithmic scale of the relative quantity C/C_{max} is used. The results of the model are in agreement with previous studies conducted in the area (Philippopoulos *et al.,* 2007, 2009; Deligiorgi *et al.,* 2009a; Philippopoulos *et al.,* 2012).
The first case corresponds to the 1st of April 2005, where a strong Northerly flow is observed at the SOU station. The main synoptic characteristic is the passage of a cold front, which moves Southwards. Furthermore, the Northerly flow results from the combination of an anticyclone in central Europe with a low system in Eastern Turkey and is enhanced during the evening (Figure 7a). The plume, as a result of the strong flow, is transferred to the wind direction, following the terrain. Due to its high kinetic energy, the plume is concentrated around the main transfer axis, without being trapped in the valley of Chania (Figure 7a).

In the second case of the 26th November 2004, the regional wind flow is defined by the combination of a high-pressure system located at the northwest of Greece in central Europe and the low-pressure system in the Eastern Mediterranean over Cyprus. The wind flow over the study area is from the northern sector and medium intensity winds are observed throughout the day (Figure 7b). According to this figure a significant amount of the plume is trapped in the Chania valley and the higher concentrations are observed in the southeast and in particular at the foot of the White Mountains.

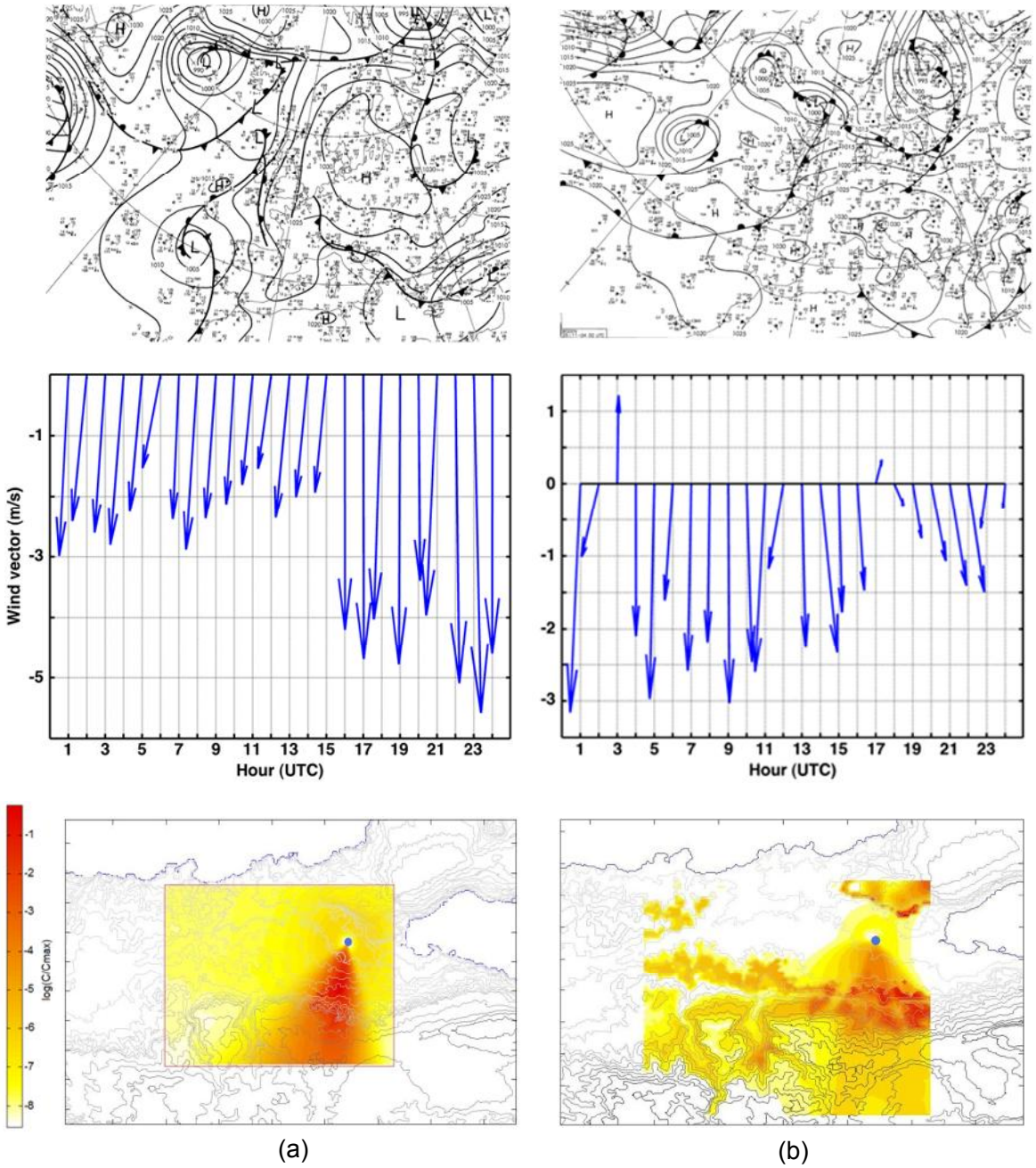

Figure 7. Surface pressure maps for 00:00 UTC, daily wind evolution at SOU station and AERMOD's ground level predicted SO_2 concentrations on (a) 01/04/2005 and (b) 26/11/2004. PPC location is indicated with a blue dot

The synoptic condition of the third case of the 11th August 2004 is characterized by a rather smooth high-pressure field, which interacts with a relatively weak low-pressure system on the east of Crete, over Cyprus. The wind flow, according to the surface observations at the SOU site, is from the west-northwest during the night and the early morning hours which later during the day shift to a medium intensity southeastern flow (Figure 8a). The maximum SO_2 concentrations are also observed at the foot of the White Mountains and at the foothills at the west of the Chania plain. In addition, a part of the plume is transported from the northeasterly flow to the south of the power plant, towards the Chania city. Northeasterly flows are relatively infrequent but can lead to air pollution episodes in the greater area of Chania city (Figure 8a).

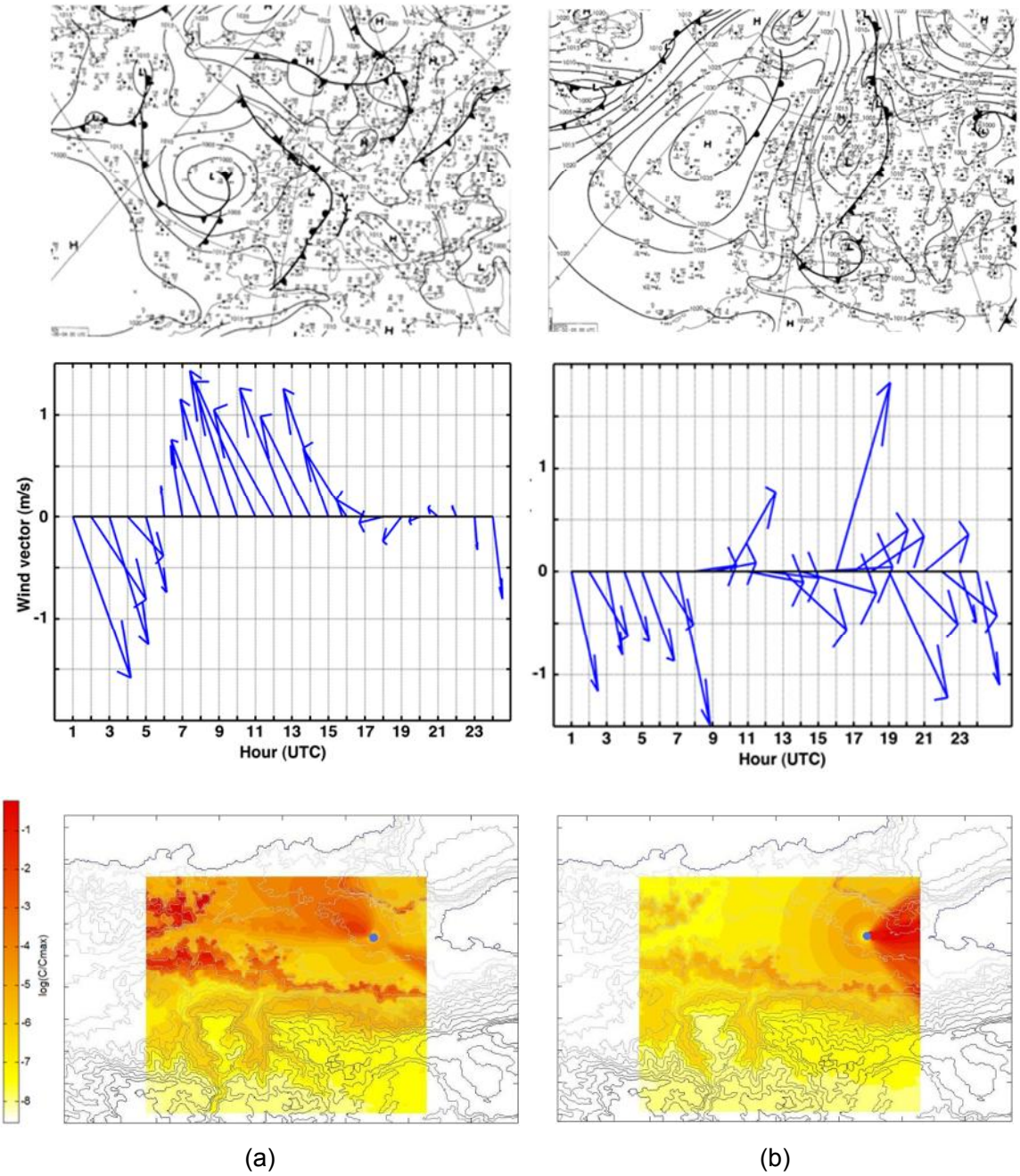

(a) (b)

Figure 8. Similar to Figure 7 for case studies on (a) 11/08/2004 and (b) 20/02/2005

In the fourth case during the 20th February 2005, the area under study is under the influence of a low-pressure system, located on the Gulf of Genoa, which leads to a westerly flow at the Chania plain (Figure 8b). Low levels of background ground level SO_2 concentrations are observed throughout the study area while the plume is mainly transported to the east. The lack of physical boundaries across the plume main transport axis results to the lack of pollution entrapment in the Chania plain.

The synoptic condition of the fifth case of 21st June 2005 is a characteristic summer-time case where the pressure systems are attenuated, leading to smooth pressure fields that favor the development of local flows in the island of Crete. During the night the flow is weak but under the influence of the sea breeze, the flow during midday and afternoon hours is enhanced and is mainly from the northern sector (Figure 9a). The entrapment of the plume is observed in the south of the Chania plain and the characteristic feature of this case study is the penetration of the pollutants into the two narrow openings of the White Mountains, a fact which is represented with clarity in Figure 9a.

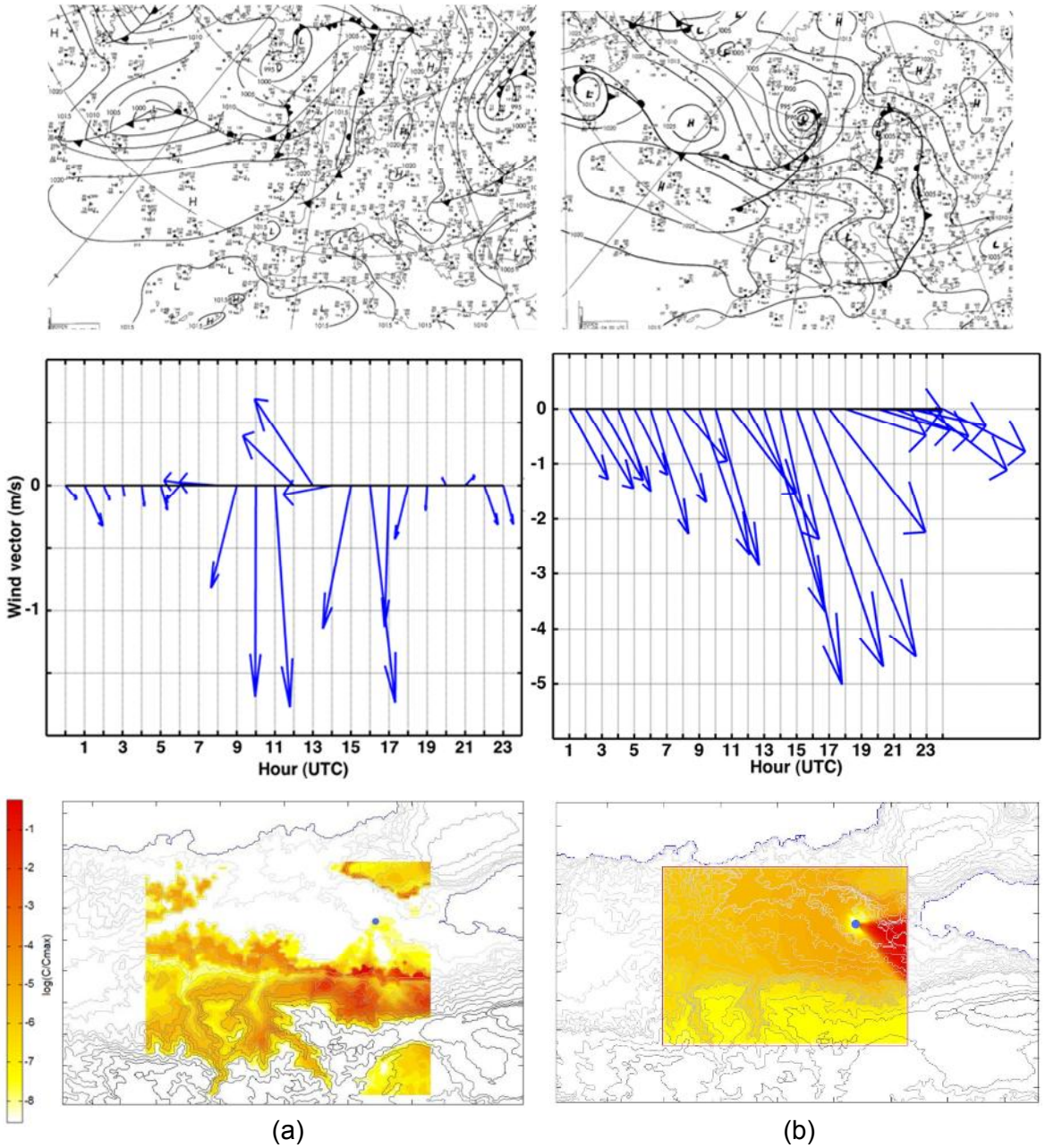

Figure 9. Similar to Figure 7 for case studies on (a) 21/06/2005 and (b) 27/08/2004

The sixth case corresponds to the 27th August 2004. This day is characterized by a combination of a relatively high pressure system in the central Mediterranean and Greece with a relative shallow low system in the Southeastern Turkey. Such a system is mainly observed during the warm period of the year. This synoptic condition leads to a background West-northwestern flow, which is enhanced during midday hours under the influence of the sea breeze circulation cell (Figure 9b). This case corresponds to a group of days where air pollution concentrations are strongly influenced by the interaction of mesoscale flow (i.e. sea-breeze) with synoptic gradient winds. The relatively strong flow, especially during the midday hours, results in the transfer of the plume along the prevalent direction with relatively low horizontal dispersion. The flat terrain at the eastern part of the power plant contributes to the above mentioned dispersion pattern (Figure 9b).

5. CONCLUSIONS

The results of this study prove that the greater area of the Chania plain is non-homogeneous in terms of wind speed, wind direction, atmospheric stability and mixing height. Taking into account the

proximity and the similarities in land-usage and land-cover characteristics between the power plant and SOU station, an initial estimation of this sub-area is made. AERMOD modeling system was applied for the Southeastern part of the Chania plain and for days with well established wind flows. The ground level daily averaged sulfur dioxide concentrations were obtained. The selection of days was based on the analysis of the surface pressure maps at 00:00 UTC and the wind measurements at the six experimental sites. Case studies are presented, which reveal the dispersion patterns of sulphur dioxide in the region. The effect of topography and the complexity of wind circulation patterns lead to a number of dispersion patterns in the region. Under weak wind regimes the higher concentrations are predicted at the roots of the White Mountains, while under strong wind regimes the top-end concentrations are found along the plume centerline.

REFERENCES

Bailey D.T. (2000), Meteorological Monitoring Guidance for Regulatory Modeling Applications, Report, U.S. Environmental Protection Agency.

Bluett J., Gimson N., Fisher G., Heydenrych C., Freeman T. and Godfrey J. (2004), Good Practice Guide for Atmospheric Dispersion Modelling, Ministry for the Environment, Wellington, New Zealand.

Borrego C., Tchepel O., Costa A. M., Amorim J. H. and Miranda A.I. (2003), Emission and dispersion modeling of Lisbon air quality at local scale, *Atmospheric Environment*, **37**, 5197-5205.

Briggs G.A. (1971), Some recent analyses of plume rise observation," In Proceedings of 2nd Int. Clean Air Congress, New York.

Briggs G.A. (1972), Discussion: chimney plumes in neutral and stable surroundings, *Atmospheric Environment*, **6**, 507-510.

Cheng S.Y., Huang G.H., Chakma A., Hao R.X., Liu L. and Zhang X.H. (2001), Estimation of Atmospheric Stability Mixing Heights using data from Airport Meteorological Stations, *J. Environ. Sci. Health*, **A36**(4), 521-532.

Cimorelli, A. J., Perry S. G., Venkatram A., Weil J. C., Paine R. J., Wilson R. B., Lee R. F. and Peters W. D. (2003), AERMOD description of model formulation, U.S. Environmental Protection Agency.

Davitashvili T. (2009), Mathematical Modeling Pollution From Heavy Traffic in Tbilisi Streets, *WSEAS Trans. on Environment and Development*, **5**, 498-507.

Deligiorgi D., Tzanakou M., Philippopoulos K. and Karvounis G. (2008), Study of the main synoptic patterns in the broader area of Chania Crete and their correlation with the main meteorological parameters, Proceeding of the 9th International Conference on Meteorology and Atmospheric Physics, COMECAP 2008, Thessaloniki, Greece, 59-66.

Deligiorgi D., Philippopoulos K., Karvounis G. and Tzanakou M. (2009a), Identification of pollution dispersion patterns in complex terrain using AERMOD modelling system, *International Journal of Energy and Environment*, **3**(3), 143-150.

Deligiorgi D., K. Philippopoulos, M. Tzanakou and Karvounis G. (2009b), Study of the influence of synoptic scale flows on sea breeze circulation in the greater area of Chania, Greece, Proceedings of the 11th International Conference on Environmental Science and Technology (CEST2009), Chania, Crete, Greece, A 212-219.

Gualtieri G., Busillo C. and Calastrini F. (2008), Modelling emission scenarios variations: an inert-mode CALGRID long-term application over the Florence metropolitan area to improve PM10–related air quality standards, *WSEAS Trans. on Environment and Development*, **4**, 970-981.

Hazelton M.L. and Turlach B.A. (2007), Reweighted Kernel Density Estimation, *Computational Statistics & Data Analysis*, **51**(6), 3057-3069.

Holmes N.S. and Morawska L. (2006), A review of dispersion modelling and its application to the dispersion of particles: An overview of different dispersion models, *Atmospheric Environment*, **40**, 5902-5928.

Karvounis G., Deligiorgi D., and Philippopoulos K. (2007), On the sensitivity of AERMOD to surface parameters under various anemological conditions, Proceedings of the 11th International Conference on Harmonisation within Atmospheric Dispersion Modelling for Regulatory Purposes, Cambridge, UK, 43-47.

Knoderer C. (2004), CRPAQS Surface and Aloft Meteorological Representativeness, URL: http://www.sonomatechdata.com/crpaqsmetrep/index.cfm

Latini G.R., Cocci G. and Passerini G. (2002), The Optimal Choice of AERMOD Input Data in Complex Areas, *Air Pollution Modeling and Its Application*, **XV**, 513-514.

Moussiopoulos N., Papagrigoriou S., Bartzis J.G., Nester K., Van den Bergh H. and Theodoridis G. (2000), Forecasting air quality in the Greater Athens area for the year 2004: an intercomparison of the results of four different dispersion models, *Int. J. of Environment and Pollution*, **14**, 343-353.

Nappo C.J., Caneill J.Y., Furman R.W., Gifford F.A., Kaimal J.C., Kramer M.L., Lockhart T.J., Pendergas M.M., Pielke R.A., Randerson D., Shreffler J.H. and Wyngaard J.C. (1982), The Workshop on the Representativeness of Meteorological Observations, *Bull. Am. Meteorol. Soc*., **63**, 761-764.

Pasquill F. (1961), The estimation of the dispersion of windborne material, *Meteorol. Mag*., **90**, 33-49.

Philippopoulos K., Karvounis G. and Deligiorgi D. (2007), Meteorological representivity analysis and modelling the atmospheric dispersion of a power plant plume, Proceedings of the 10th International Conference on Environmental Science and Technology, CEST2007, Kos island, Greece, B 618-625.

Philippopoulos K., Deligiorgi D., Karvounis G. and Tzanakou M. (2009), Pollution dispersion modelling at Chania, Greece, under various meteorological conditions, Proceedings of the 5th International Conference on Energy, Environment, Ecosystems and Sustainable Development (EEESD'09), Vouliagmeni, Athens, Greece, 133-138.

Philippopoulos K., Deligiorgi D. and Karvounis G. (2012), Wind speed distribution modelling in the greater area of Chania, Greece, *International Journal of Green Energy*, **9**(2), 174-193.

San Jose R., Perez J. L. and Gonzalez R. M. (2006), Air Quality CFD and Mesoscale Modelling Simulations: Madrid Case Study, *WSEAS Trans. on Environment and Development*, **2**, 1291-1296.

Turner D.B. (1964), A diffusion model for an urban area, *J. Appl. Meteor*., **3**, 83-91.

Ulke A.G. and Mazzeo N.A. (1998), Climatological aspects of the daytime mixing height in Buenos Aires City, Argentina, *Atmospheric Environment*, **32**(9), 1615-1622.

Venkatram A. (2001), Challenges of Air Pollution Modeling and its Application in the Next Millennium, *Air Pollution Modeling and Its Application*, **XIV**, 613-630.